Cellular growth near absolute stability

K. Brattkus and S. H. Davis
Department of Engineering Sciences and Applied Mathematics, The Technological Institute, Northwestern University, Evanston, Illinois 60208
(Received 15 April 1988)

We derive a strongly nonlinear evolution equation for the interface of a directionally solidified binary alloy when surface energies are large. This equation includes interfacial acceleration and the nonlinear effects of surface tension. Bifurcation analysis on this equation reveals that planar interfaces immediately develop three-dimensional structure, and, when the segregation coefficient is near unity, stable hexagonal solutions are found.

I. INTRODUCTION

Three-dimensional free-surface problems often become analytically tractable under a separation of scales. If surface deflection is known to vary slowly along the surface, an evolution equation for the interface may be derived which governs the dynamics of long waves. This approach can also be used to describe surface instabilities if critical disturbances are known to have asymptotically large wavelengths.

Recently, several evolution equations of this type have been derived for solid/liquid interfaces established during the directional solidification of a binary alloy.[1-5] Here, a planar surface of phase change, which advances uniformly through a fixed temperature gradient, is subject to a cellular instability due to solute rejection. The amount of solute rejected at the freezing interface is governed by the segregation coefficient, $k = C_S/C_L$, which relates the concentration of solute on either side of the interface. From the linear theory,[6] Sivashinsky[1] recognized that as k diminishes, instabilities first develop to disturbances with very large wavelengths. The resulting evolution equation has since then been modified to include the effects of latent heat,[2] solute bouyancy,[3] and anisotropic attachment kinetics.[4]

A local theory on the two-dimensional version of this evolution equation reveals that the bifurcation to unstable cells[4] is subcritical in nature. Numerical integration[3] also shows subcritical bifurcation and suggests that solutions to the evolution equation develop cusp singularities in finite time. The development of finite-time cusp singularities in solutions to the evolution equation has now been proved for specific boundary conditions.[7] The fact that bifurcation is subcritical for small segregation coefficients[8] explains why the small k evolution equation does not give stabilization to cellular structures.

As an alternative to attempting *ad hoc* procedures for the inclusion of higher-order terms into this evolution equation for small k,[9,10] one can consider other limits which also produce long-wave instabilities. The limit of small temperature gradients has been investigated by Novick-Cohen,[5] who requires attachment kinetics to stabilize against the runaway. The resulting evolution equation is the familiar Kuramoto-Sivashinsky equation.

In the present paper we also consider the limit of small temperature gradients but find that we *can* stabilize with surface energy. Specifically, we restrict our attention to systems near the absolute stability limit; higher surface energies than the critical value result in the planar interface being stable to small disturbances. In this limit we were able to derive a new, strongly nonlinear evolution equation which contains supercritical bifurcation, interesting three-dimensional cellular pattern selection, and might even contain the onset of time-variable states.

II. FORMULATION

The unidirectional solidification of a dilute binary alloy involves the pulling of an alloy with a constant speed V through two fixed temperature sources. One of these melts the alloy while the other freezes it. At some point between the two sources, a solid-liquid interface is established at a mean position fixed with respect to both temperature sources. The melt is continually solidified at a constant rate V and if V is small enough, the interface between the solid and liquid phase remains planar.

The concentration of the secondary component in the binary alloy, c^*, has a value of c_0^* in the static melt, far from the interface. We consider an infinite one-sided model and neglect the diffusion of solute in the solid.[6] We also adopt the "frozen temperature" approximation[11] and assume that (i) the thermal conductivities of both the solid and the liquid are equal, (ii) the thermal diffusivity, κ, is much larger than D, the diffusivity of solute in the liquid, and (iii) the latent heat is negligible. Under these assumptions, the temperature field is fixed independent of the solute concentration, and is given by

$$T = T_0 + Gz^* \ . \tag{2.1}$$

Here z^* is the coordinate in the direction of growth, fixed on the interface, G is the imposed temperature gradient, and T_0 is the temperature of a planar interface (Fig. 1). The temperature field now decouples from the problem and the solidification process is completely governed by the distribution of solute. Since latent heat production is enhanced as pulling velocities increase, the linear temperature profile is quite often a poor approximation for rapid solidification processes. Realistic models in this case re-

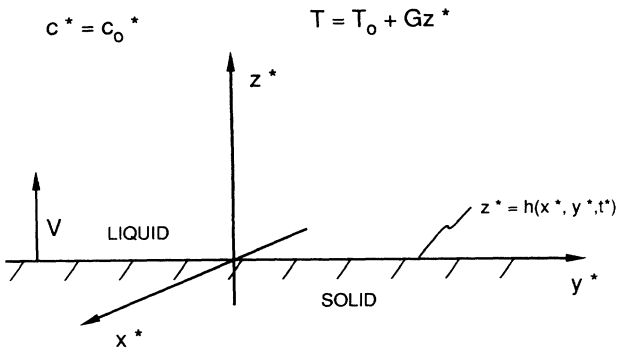

FIG. 1. Directional solidification into a binary alloy of solute concentration c_0^* with a constant velocity V.

quire a complete description of both the thermal and solute fields.

If lengths are scaled on the diffusional scale, D/V, and a nondimensional solute, c, is defined by

$$c^*=[1+(k-1)c]c_0^*/k \ , \tag{2.2}$$

then in the frame of reference moving with the interface, the scaled equations determining the solute concentration and the interface position, $h(x,y,t)$, are as follows:

$$\nabla^2 c+c_{zz}+c_z=c_t \ , \tag{2.3}$$

$$[1+(k-1)c](1+h_t)=c_z-\nabla h\cdot\nabla c, \quad z=h \ , \tag{2.4a}$$

$$c-M^{-1}h+\Gamma\nabla\cdot[\nabla h/(1+|\nabla h|^2)^{1/2}]=0, \quad z=h \ , \tag{2.4b}$$

$$c=1, \quad z=\infty \ , \tag{2.5}$$

where ∇ and ∇^2 are the two-dimensional gradient and Laplacian operators, respectively. The boundary condition (2.4a) governs conservation of solute across the interface and condition (2.4b) is a scaled version of the Gibbs-Thomson relation. The three nondimensional parameters are the segregation coefficient k, a morphological parameter M,

$$M=\frac{m(1-k)c_0^*V}{kGD} \ ; \tag{2.6}$$

and the scaled surface energy Γ,

$$\Gamma=\frac{kT_MV(\gamma/L_V)}{c_0^*m(1-k)D} \ . \tag{2.7}$$

Here m is the slope of the liquidus, γ is the surface energy per unit area, and L_V is the latent heat per unit volume.

III. BASIC STATE AND LINEAR STABILITY

As mentioned previously, when pulling velocities are low, the interface is a planar, uniformly translating front. This behavior is represented by the basic state solution to the system (2.3)–(2.5) as follows:

$$h=h_0=0 \ , \tag{3.1a}$$

$$c=c_0=1-e^{-z} \ . \tag{3.1b}$$

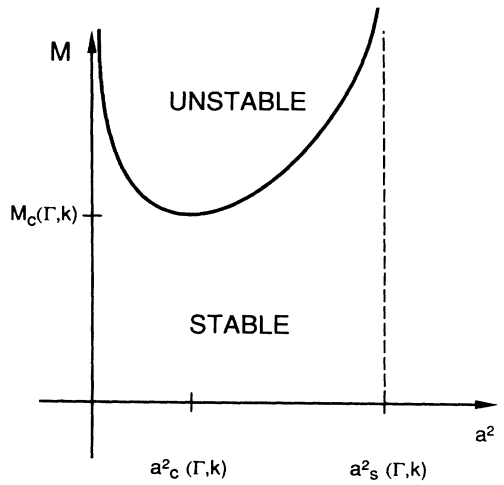

FIG. 2. Typical marginal stability diagram for planar growth. Infinitesimal disturbances with wave number a_c grow exponentially in time when $M>M_c$. All disturbances with $a>a_s$ are absolutely stable and decay for any $M>0$.

The linear instability of this solution is examined by allowing infinitesimal disturbances to the basic state and expanding them in normal modes as follows:

$$\begin{bmatrix} h \\ c \end{bmatrix}=\begin{bmatrix} 0 \\ 1-e^{-z} \end{bmatrix}+\begin{bmatrix} H \\ c(z) \end{bmatrix}e^{\sigma t+i\mathbf{a}\cdot\mathbf{r}} \ , \tag{3.2}$$

where

$$\mathbf{a}=(a_x,a_y), \quad \mathbf{r}=(x,y) \ . \tag{3.3}$$

When we linearize (2.3)–(2.5) about (3.1) and (3.2) and solve the resulting eigenvalue problem for the growth rate σ, we find a simplified version of the characteristic equation derived by Mullins and Sekerka,[6] viz.,

$$\sigma=(1-M^{-1}-a^2\Gamma)[(\tfrac{1}{4}+\sigma+a^2)^{1/2}+k-\tfrac{1}{2}]-k \ , \tag{3.4}$$

where $a=|\mathbf{a}|$.

If we treat M as the control parameter, then a typical marginal stability curve separating regions of instability ($\mathrm{Re}\sigma<0$) from regions of instability ($\mathrm{Re}\sigma>0$), is shown in Fig. 2. When $M>M_c(\Gamma,k)$, the planar interface is linearly unstable to an annulus of wave vectors, including the circle of wave vectors with $a=a_c(\Gamma,k)$. This morphological instability evolves to a cellular pattern in the solidification front as we shall show in Sec. VI for a limiting case. (See also Refs. 8 and 12).

IV. ABSOLUTE STABILITY

An interesting feature of Fig. 2 is the presence of a short-wavelength cutoff. For disturbances with large enough wave numbers $a>a_s(\Gamma,k)$, the stabilizing action of surface energy overcomes the destabilizing influence of the solute gradients. These disturbances are stable for all values of M (all pulling velocities) and are described as being *absolutely stable.*[6]

The critical parameters derived from (3.4) vary with both the surface energy Γ and the segregation coefficient

k. It has long been recognized[6] that there exists a critical value of the surface energy, which turns out to be $\Gamma_s = 1/k$, such that when $\Gamma > \Gamma_s$, $a_s(\Gamma,k)=0$ and the system is stable to all infinitesimal disturbances for all pulling velocities. If Γ is slightly less than $1/k$, the planar solution loses stability but only at very large values of M; large solute gradients are required. It is not difficult to show that

$$\lim_{\Gamma\to\Gamma_s^-} a_c(\Gamma,k)=0 , \tag{4.1}$$

and

$$\lim_{\Gamma\to\Gamma_s^-} M_c^{-1}(\Gamma,k)=0 . \tag{4.2}$$

Therefore, as the surface energy approaches the value of $1/k$ from below, the wave numbers of the most unstable modes are very small. When $M > M_c \gg 1$, the planar interface loses stability to modes which vary slowly in the horizontal directions, and a long-wavelength instability results.

We noted that $a_s(\Gamma,k)=0$ when Γ is larger than $1/k$. The expected result that

$$\lim_{\Gamma\to\Gamma_s^-} a_s(\Gamma,k)=0 , \tag{4.3}$$

is also easily established. If we remember that disturbances with wave numbers larger than a_s are always stable, the conclusion is much stronger. As Γ approaches $1/k$ from below, *all* unstable disturbances have small wave numbers and thus vary slowly in space. We show in Sec. V that this observation has important implications in the nonlinear development of the instability.

The stability boundaries can be summarized clearly by plotting M_c^{-1} versus Γ for fixed k as shown in Fig. 3. When $\Gamma=0$, $M_c^{-1}=1$, and $M_c^{-1}=0$ for $\Gamma=\Gamma_s$. Along the curve separating stability from instability, a_c decreases from infinity monotonically to zero as Γ tends from zero to Γ_s.

If the difference between Γ and $1/k$ is defined as a

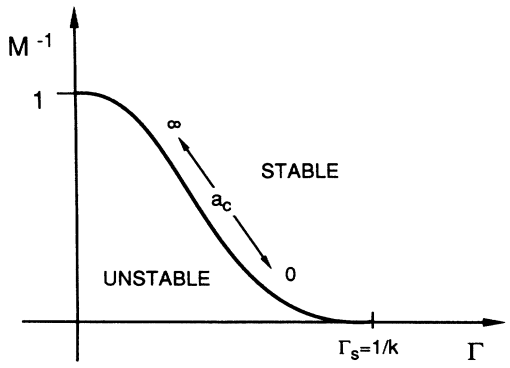

FIG. 3. The stability of planar growth as a function of surface energy. If $\Gamma=0$, then $M_c=1$ and the most critical disturbance has zero wavelength. As Γ increases to $\Gamma_s=1/k$, both the wavelength of the critical disturbance and M_c increase monotonically to infinity. When $\Gamma > \Gamma_s$ planar growth is absolutely stable and there is no instability.

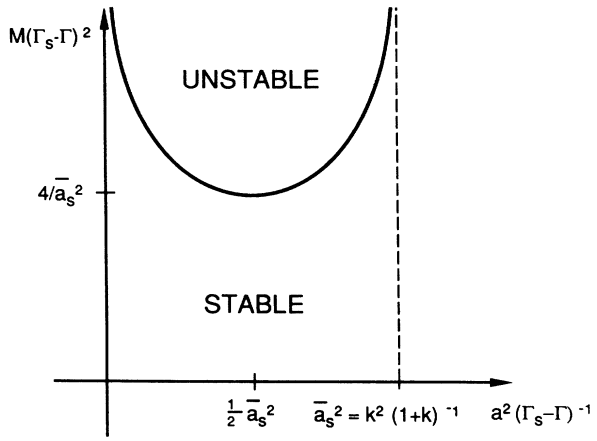

FIG. 4. Marginal stability given by Eq. (4.5) when $\Gamma_s-\Gamma$ is small. As Γ tends to Γ_s both a_c^2 and a_s^2 are $O(\Gamma_s-\Gamma)$ while M_c is $O((\Gamma_s-\Gamma)^{-2})$.

small parameter ϵ, we find that the following scalings are appropriate near marginal conditions:

$$\Gamma=\frac{1}{k}-\epsilon , \tag{4.4a}$$

$$M^{-1}=\bar{M}^{-1}\epsilon^2 , \tag{4.4b}$$

$$a=\epsilon^{1/2}\bar{a} , \tag{4.4c}$$

$$\sigma=\epsilon\bar{\sigma} , \tag{4.4d}$$

where all barred quantities and k are assumed unit order as $\epsilon\to 0$. These scaled variables lead to an approximate characteristic equation for the linear stability problem of the planar interface as follows:

$$\bar{\sigma}^2+\left[2+\frac{1}{k}\right]\bar{a}^2\bar{\sigma} + \left[k\bar{M}^{-1}-k\bar{a}^2+\bar{a}^4\left[1+\frac{1}{k}\right]\right]=0 . \tag{4.5}$$

The marginal stability curve for (4.5) is presented in Fig. 4. Notice that Eq. (4.5) is quadratic in $\bar{\sigma}$.

V. STRONGLY NONLINEAR ANALYSIS

To examine the nonlinear development of the unstable long waves near the absolute stability limit, again define

$$\Gamma=1/k-\epsilon \tag{5.1}$$

and rescale the full system (2.3)–(2.5) on those scalings motivated by the linear theory of Sec. IV as follows:

$$(x,y,z)=(\epsilon^{-1/2}X,\epsilon^{-1/2}Y,Z) , \tag{5.2a}$$

$$t=\epsilon^{-1}T , \tag{5.2b}$$

$$M=\bar{M}/\epsilon^2 , \tag{5.2c}$$

where k, $\bar{M}$, and derivatives in uppercase variables are assumed unit order as $\epsilon \to 0$. Note that although the morphological parameter M is large, we have *not* restricted it to be near its critical value M_c. Since $M - M_c$ may be large, the interface deflection is not necessarily small and we retain unit-order deflections and concentrations:

$$h(x,y,t) = H(X,Y,T), \quad c(x,y,z,t) = C(X,Y,Z,T) . \tag{5.3}$$

Since the interface may have large amplitude deflections, we simplify the problem by introducing the coordinate transformation, $\zeta = Z - H(X,Y,T)$, and write the rescaled governing equations as follows:

$$\epsilon(C_T - H_T C_\zeta) = \epsilon(\nabla^2 C - 2\nabla C_\zeta \cdot \nabla H - C_\zeta \nabla^2 H + C_{\zeta\zeta}|\nabla H|^2) + C_{\zeta\zeta} + C_\zeta, \quad \zeta > 0 , \tag{5.4}$$

$$\left.\begin{aligned} &[1+(k-1)C](1+\epsilon H_T) = C_\zeta - \epsilon(\nabla C \cdot \nabla H - C_\zeta |\nabla H|^2) \\ &C - \epsilon^2 \bar{M}^{-1} H + \epsilon \left(\frac{1}{k} - \epsilon\right) \nabla \cdot [\nabla H / (1+\epsilon|\nabla H|^2)^{1/2}] = 0 \end{aligned}\right\}, \quad \zeta = 0 , \tag{5.5}$$

$$C = 1, \quad \zeta = \infty . \tag{5.6}$$

Although the diffusion equation (5.4) appears to be more complicated, the application of the boundary conditions on $\zeta = 0$ instead of $Z = H$ substantially simplifies the analysis. We now seek solutions to (5.4)–(5.6) in powers of ϵ as follows:

$$C = C_0 + \epsilon C_1 + \epsilon^2 C_2 + \cdots , \tag{5.7a}$$

$$H = H_0 + \epsilon H_1 + \cdots . \tag{5.7b}$$

The problem for C_0 at leading order in ϵ becomes

$$C_{0\zeta\zeta} + C_{0\zeta} = 0, \quad \zeta > 0 , \tag{5.8}$$

$$\left.\begin{aligned} &C_{0\zeta} + (1-k)C_0 = 1 \\ &C_0 = 0 \end{aligned}\right\}, \quad \zeta = 0 , \tag{5.9a}$$

$$C_0 = 1, \quad \zeta = \infty , \tag{5.9b}$$

which has the solution

$$C_0 = 1 - e^{-\zeta} . \tag{5.10}$$

Note that this solution is the basic state when $H = 0$. At the next order in ϵ the problem for C_1 becomes

$$C_{1\zeta\zeta} + C_{1\zeta} = (\nabla^2 H_0 + |\nabla H_0|^2 - H_{0T}) e^{-\zeta}, \quad \zeta > 0 , \tag{5.11}$$

$$\left.\begin{aligned} &C_{1\zeta} + (1+k)C_{1\zeta} = H_{0T} - |\nabla H|^2 \\ &C_1 = -\frac{1}{k}\nabla^2 H_0 \end{aligned}\right\}, \quad \zeta = 0 , \tag{5.12}$$

$$C_1 = 0, \quad \zeta = \infty , \tag{5.13}$$

and has the solution

$$C_1 = -\frac{e^{-\zeta}}{k}\nabla^2 H_0 + (H_{0T} - \nabla^2 H_0 - |\nabla H_0|^2)\zeta e^{-\zeta} . \tag{5.14}$$

Proceeding to the next highest order we must solve

$$C_{2\zeta\zeta} + C_{2\zeta} = C_{1T} - H_{0T} C_{1\zeta} - H_{1T} C_{0\zeta} - \nabla^2 C_1 + 2\nabla C_{1\zeta} \cdot \nabla H_0 + C_{0\zeta}\nabla^2 H_1 + C_{1\zeta}\nabla^2 H_0 - C_{1\zeta\zeta}|\nabla H_0|^2 - 2C_{0\zeta\zeta}\nabla H_0 \cdot \nabla H_1, \quad \zeta > 0 , \tag{5.15}$$

$$\left.\begin{aligned} &C_{2\zeta} + (1-k)C_2 = H_{1T} + (k-1)C_1 H_{0T} + C_{1\zeta}|\nabla H_0|^2 + C_{0\zeta}|\nabla H_1|^2 - \nabla C_1 \cdot \nabla H_0 \\ &C_2 = \bar{M}^{-1} H_0 - \frac{1}{k}\nabla^2 H_1 + \nabla^2 H_0 + \frac{1}{2k}\nabla \cdot (\nabla H |\nabla H|^2) \end{aligned}\right\} \quad \zeta = 0 , \tag{5.16}$$

$$C_2 = 0, \quad \zeta = \infty . \tag{5.17}$$

The existence of a solution to (5.15)–(5.17) places a restriction on H_0. Solutions exist only if the system satisfies an orthogonality condition, which forces H_0 to obey the following long-wave evolution equation:

$$H_{0TT} - \left(2 + \frac{1}{k}\right)\nabla^2 H_{0T} + \left(1 + \frac{1}{k}\right)\nabla^4 H_0 + k\nabla^2 H_0 + k\bar{M}^{-1} H_0 = H_{0T}\nabla^2 H_0 + |\nabla H_0|_T^2 - \nabla^2(|\nabla H_0|^2) - \frac{1}{k}\nabla \cdot (\nabla^2 H_0 \nabla H_0) - \tfrac{1}{2}\nabla \cdot (\nabla H_0 |\nabla H_0|^2) . \tag{5.18}$$

At this point we have significantly simplified the original free-boundary problem (2.3)–(2.5) and can locate the position of the boundary at any time T by an appropriate integration of (5.18).

There are several features which distinguish the evolution equation (5.18) from all others[1–5] previously derived for directional solidification. First, the equation is *strongly nonlinear;* both quadratic and cubic nonlinearities appear. Their appearance is a reflection of possible large amplitude variations in the interface. The derivation of a strongly nonlinear evolution equation is only possible when *all* unstable disturbances have wave numbers that are asymptotically small; such is the case near the absolute stability limit.

A second important difference is that (5.18) includes the effects of interfacial acceleration. As can be observed from (5.4) and (5.5), the derivatives, which are second order in time, were foreshadowed by Eq. (4.5) being quadratic in $\bar{\sigma}$ and reflects a lack of quasistationarity in the solute field. The moving front simultaneously affects the solute flux at the front [Eq. (5.5a)] and the rate of diffusion of solute away from the front [Eq. (5.4)]. This should be contrasted to the weakly nonlinear analyses which produce evolution equations that are first order in time and have quasistatic solute fields; interface velocities affect the solute flux at the front which must then steadily diffuse into the melt.

Finally we see that the evolution equation (5.18) gives a long-wave theory for directional solidification which consistently includes the nonlinear effects of surface tension; these effects are responsible for the cubic terms.

Before continuing with an analysis on the evolution equation, we rescale to a more appropriate form as follows:

$$F=\frac{1}{(2k+1)}H_0,\quad (\xi,\eta)=\frac{k^{3/2}}{(2k+1)}(X,Y)\ ,$$
$$\tau=\frac{k^2}{(2k+1)}T\ . \tag{5.19}$$

Equation (5.18) then takes the following form:

$$F_{\tau\tau}-\nabla^2F_\tau+\tfrac{1}{4}(1-\nu^2)\nabla^4F+\nabla^2F+\mu^{-1}F$$
$$=F_\tau\nabla^2F+|\nabla F|^2_\tau-\tfrac{1}{2}(1-\nu)\nabla^2(|\nabla F|^2)-\nu\nabla\cdot(\nabla F\nabla^2F)$$
$$-\tfrac{1}{2}\nabla\cdot(\nabla F|\nabla F|^2)\ , \tag{5.20}$$

where

$$\nu=\frac{1}{1+2k},\quad \mu^{-1}=\frac{(2k+1)^2}{k^3}\overline{M}^{-1}\ . \tag{5.21}$$

In Sec. VI we study the transition from planar to cellular states using the two parameter equation (5.20).

VI. TRANSITION AND PATTERN

Near absolute stability, the solidification process evolves on the long spatial and slow time scales given in (5.2) The nonlinear dynamics of the interface is then governed by Eq. (5.20), which can be used to describe the nonlinear features of the transition from planar to cellular states, i.e., the morphological instability.

The solidification of a planar front is represented by $F=0$. If we investigate the stability of this solution to infinitesimal disturbances as was done in Sec. III, we find a rescaled version of the characteristic equation (4.5). The critical parameters which correspond to an onset of instability are given by $\mu_c=1-\nu^2$ and $a_c^2=2\mu_c^{-1}$.

If critical conditions are slightly exceeded, the two-dimensional, weakly nonlinear development of the instability may be followed using a variety of techniques.[13–15] The results of such analyses on the η-independent evolution equation show *supercritical bifurcation* to cellular solutions. Such behavior is consistent with the conclusions of Wollkind and Segel[8] who perform similar computations on the full system (2.3)–(2.5).

When $\mu\geq\mu_c$, we expect that an initially flat interface will stabilize into a two-dimensional steady cellular pattern. The effects of nonlinearity on this solution are investigated by numerical integration of the steady, η-independent version of the evolution equation, the results of which are shown in Fig. 5. Here we have imposed

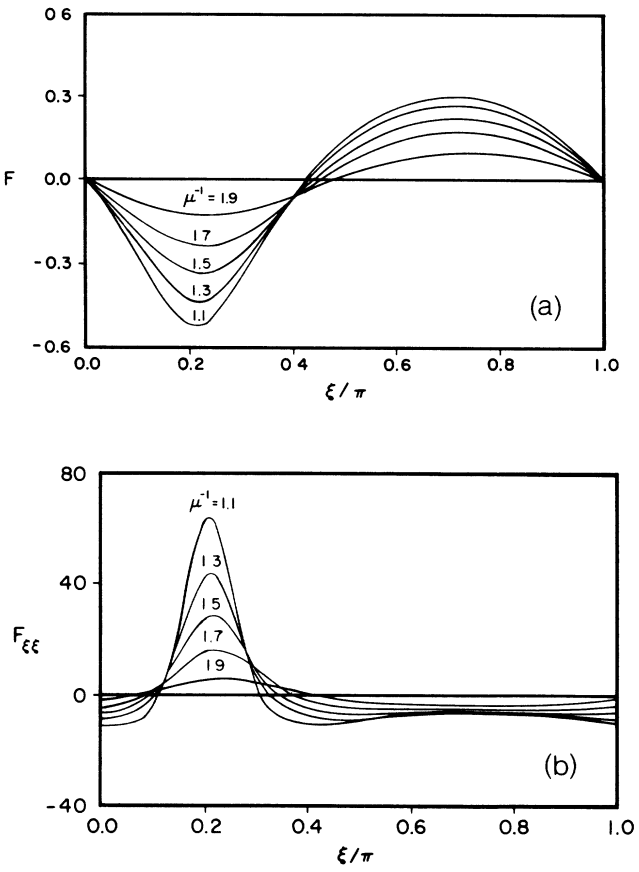

FIG. 5. (a) Position of the steady, solid-liquid interface found by integrating the η- and τ-independent version of Eq. (5.20) with periodic boundary conditions for $\nu=1/\sqrt{2}$. (b) The distribution of solute along the interface is given by

$$c_l^*/c_0^*=1+\epsilon[(1-k)(1+2k)/k^3]F_{\xi\xi}+O(\epsilon^2)\ .$$

Even though the analysis is strongly nonlinear and F is of unit order, solute varies by only an $O(\epsilon)$ amount over the interface.

periodic boundary conditions and fixed the wavelength at $2\pi/a_c$. The value of ν is taken as $\frac{1}{2}\sqrt{2}$ ($k\simeq 0.2$) which gives $\mu_c=\frac{1}{2}$. As μ increases past μ_c, the initially sinusoidal interface develops asymmetries which correspond to the root and tip regions of a cell as shown in Fig. 5(a). The corresponding concentration of solute at the interface is found directly from Eq. (5.14) and is shown in Fig. 5(b). It is interesting to note that although the interface deflection may be large, solute variations along the interface are not; they are proportional to ϵ.

The development of these nonlinear cells is qualitatively similar to that found in numerical models of the full two-dimensional solidification problem[16,17] and should give quantitative agreement when such models are run near the absolute stability limit. The numerical treatments involve marching forward in time, and except for certain special cases, converge to steady cells. Time dependence is an expected feature of the solidification process, dendritic growth is an example, and the inability of these two-dimensional numerical models to predict time-dependence lead Ungar and Brown[16] to postulate the existence of a precursory bifurcation to three-dimensional solutions from which time dependence may emerge. At this point, no three-dimensional and time-dependent numerical simulations have been accomplished, although three-dimensional, steady cells have recently been calculated by McFadden, Coriell, and Boisvert.[18]

The evolution equation (5.20) represents a time-dependent, three-dimensional theory and appears to be an attractive way to study possible transitions to three dimensionality and time dependence. A local theory on the η-independent version of (5.20) shows transition to steady cells which we have followed numerically for larger values of μ. We have no information on the stability of these solutions far away from $\mu=\mu_c$ although this would come from a consideration of the time-dependent form of (5.20). Instead of focusing on the stability of these two-dimensional solutions against two-dimensional disturbances, we turn to the question of whether these solutions are stable to disturbances that vary in the perpendicular direction. Is there bifurcation to three-dimensional structure?

VII. INSTABILITIES OF TWO-DIMENSIONAL CELLS

To address this issue we set $F=f_0(\xi)+f_1(\xi,\eta,\tau)$ where $f_0(\xi)$ satisfies the steady, η-independent form of (5.20) and is ξ periodic with period P. We assume that $|f_1|\ll|f_0|$ and linearize the evolution equation about f_0. This procedure gives linearized disturbances equations of the form

$$[\mathcal{L}(\mu)+\mathcal{M}]f_1=0\ , \tag{7.1a}$$

where

$$\mathcal{L}(\mu)\equiv\partial_{\tau\tau}-\nabla^2\partial_\tau+\tfrac{1}{4}(1-\nu^2)\nabla^4+\nabla^2+\mu^{-1}\ , \tag{7.1b}$$

and

$$\mathcal{M}=f_{0\xi\xi}\partial_\tau+2f_{0\xi}\partial_{\xi\tau}-\tfrac{3}{2}\partial_\xi f_{0\xi}\partial_\xi-\tfrac{1}{2}f_{0\xi}^2\partial_{\eta\eta}$$
$$-2\nu f_{0\xi\xi}\partial_{\eta\eta}-\partial_{\xi\xi}f_{0\xi}\partial_\xi-f_{0\xi}\partial_{\xi\eta\eta}\ . \tag{7.1c}$$

The operator $\mathcal{L}$ is just the linear part of (5.20) and $\mathcal{M}$ is an operator with spatially periodic coefficients. The stability problem requires a Floquet analysis of (7.1). This is greatly simplified by restricting our attention to a region near $\mu=\mu_c$ where the magnitude of f_0 is small and a local analysis give a simple asymptotic representation of f_0. If we define

$$\delta^2=\mu_c^{-1}-\mu^{-1}\ll 1\ , \tag{7.2a}$$

then

$$f_0\sim\frac{2\delta/a_c^2}{(\frac{8}{9}a_c^2-\frac{3}{2})^{1/2}}\cos a_c\xi \tag{7.2b}$$

and we take

$$f_1=\delta^2[\phi_0(\xi,\eta)+\delta\phi_1(\xi,\eta)+\cdots]e^{\sigma t} \tag{7.2c}$$

with

$$\sigma=\sigma_0+\delta\sigma_1+\delta^2\sigma_2+\cdots\ . \tag{7.2d}$$

After equating coefficients of like powers of δ, we are left to solve the consecutive problems

$$L(\mu_c)\phi_i=F_i(\phi_{i-1},\ldots,\phi_0)\ , \tag{7.3}$$

where

$$L(\mu_c)=\sigma_0^2-\sigma_0\nabla^2+\tfrac{1}{4}(1-\nu^2)\nabla^4+\nabla^2+\mu_c^{-1} \tag{7.4}$$

in order to determine whether f_1 grows or decays in time.

The homogeneous problem $L(\mu_c)\phi_0=0$ has constant coefficients so we represent solutions in terms of normal modes as follows:

$$\phi_0=e^{(\alpha\xi+\beta\eta)i}\ . \tag{7.5}$$

As expected, we find $\sigma_0<0$ unless the wave number is critical and $\alpha^2+\beta^2=a_c^2$ in which case $\sigma_0=0$. The requirement that f_1 be periodic implies that at the next order we must take $\sigma_1=0$ unless there is a resonant interaction between the disturbance and the basic state f_0, i.e., if $\beta=\pm\sqrt{\frac{3}{2}}a_c$. Excluding resonant interactions for the moment, we proceed to the third order and find that

$$\sigma_2=-\frac{1}{a_c^2}-\left[(\alpha_c^2+2\beta^2\nu)(\alpha^2+\beta^2\nu)(\alpha^2+\tfrac{1}{4}a_c^2)+a_c^2\alpha^2\left[\beta^2\nu-\frac{3a_c^2}{4}\right]\right.$$
$$\left.-\tfrac{1}{2}(3\alpha^2+\beta^2)\left[\frac{3a_c^2}{4}-\beta^2\right]^2\right]\Big/\left[\frac{3a_c^2}{4}-\beta^2\right]^2(\tfrac{8}{9}a_c^2-\tfrac{3}{2})^{1/2}\ . \tag{7.6}$$

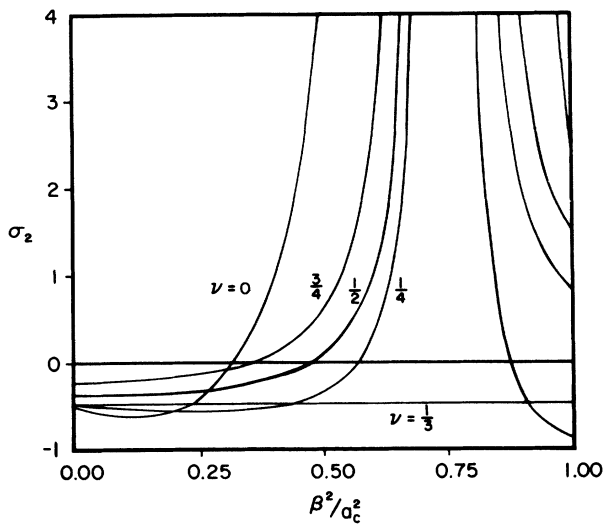

FIG. 6. The growth rate of three-dimensional disturbances to the steady, η-independent solutions of Eq. (5.20) when μ is near μ_c. When $\nu\neq\frac{1}{3}$ (or $k\neq 1$), there is a band of disturbances centered on $\beta^2=\frac{3}{4}a_c^2$ that are unstable. Here β is the wave number in the η direction.

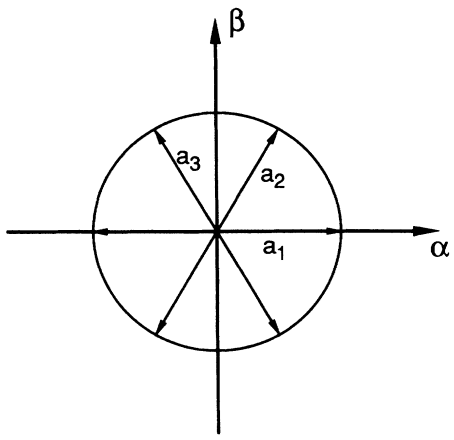

FIG. 7. The wave vectors for the six modes which are allowed to interact nonlinearly in Eq. (5.20). Here

$$\mathbf{a}_m=(\alpha\cos\tfrac{1}{3}\pi(m-1),\ \beta\sin\tfrac{1}{3}\pi(m-1))$$

and $|\mathbf{a}_m|=a_c$.

Figure 6 shows the dependence of σ_2 on β for various values of the parameter ν. It is apparent from Fig. 6 that when $\nu\neq\frac{1}{3}$, which means that $k\neq 1$, the two-dimensional solution $f_0(\xi)$ is *unstable* to three-dimensional disturbances with wave numbers centered around the resonant wave numbers, $(\alpha,\beta)=(\pm\frac{1}{2},\pm\sqrt{\frac{3}{2}})a_c$. If the system is near absolute stability and $k\neq 1$, the morphological instability immediately produces a three-dimensional structure when $\mu>\mu_c$. The case where k is nearly 1 is special and will be investigated now.

VIII. PATTERN SELECTION NEAR $k=1$

The resonant modes represent in some sense the most unstable disturbances. We return to the bifurcation analysis and assume that the bifurcating solutions at $\mu=\mu_c$ are three dimensional and consist of a combination of these six modes (Fig. 7). The amplitude of all are comparable and near bifurcation, all are assumed small. This resonant interaction approach is standard but only suggestive. We can see from Fig. 6 that the two-dimensional cells are actually unstable to a whole band of wave numbers centered around the resonant ones.

We adopt a two-timing procedure near the bifurcation point and define the small parameter δ,

$$\mu_c^{-1}-\mu^{-1}=s\delta^2,\quad s=\pm 1\ , \tag{8.1}$$

where s is $+1$ (or -1) depending upon whether the bifurcation is supercritical (or subcritical). We introduce the slow time $\bar{\tau}$,

$$\bar{\tau}=\delta^2\tau \tag{8.2}$$

and define by n the degree of closeness to unity of k:

$$\tfrac{1}{3}-\nu=n\delta\ . \tag{8.3}$$

Note from Eq. (5.21) that $\frac{1}{3}-\nu=\frac{2}{3}(k-1)/(1+2k)$ so that $n>0$ ($n<0$) refers to k larger (smaller) than unity. We expand F as follows:

$$F=\delta f_0+\delta^2 f_1+\delta^3 f_2+\cdots\ .$$

At leading order in δ, f_0 satisfies the linearized and steady version of (5.20). In reference to the preceding discussion we write,

$$f_0=\sum_{m=1}^{3}[z_m(\bar{\tau})e^{i\mathbf{a}_m\cdot\mathbf{r}}+z_m^*(\bar{\tau})e^{-i\mathbf{a}_m\cdot\mathbf{r}}]\ , \tag{8.4}$$

where z_m is a complex coefficient that depends on the slow time $\bar{\tau}$, asterisks denote complex conjugation, and wave numbers $\mathbf{a}_m$ are those associated with resonant interactions (Fig. 6). By continuing the perturbation expansion to third order we find that requirements of spatial boundedness restrict the complex z_m to satisfy the following amplitude equations:

$$\dot{z}_1=sz_1+\tfrac{3}{2}nz_2z_3-\frac{z_1}{2}[|z_1|^2+\tfrac{3}{2}(|z_2|^2+|z_3|^2)]\ , \tag{8.5a}$$

$$\dot{z}_2=sz_2+\tfrac{3}{2}nz_1z_3^*-\frac{z_2}{2}[|z_2|^2+\tfrac{3}{2}(|z_1|^2+|z_3|^2)]\ , \tag{8.5b}$$

$$\dot{z}_3=sz_3+\tfrac{3}{2}nz_1z_2^*-\frac{z_3}{2}[|z_3|^2+\tfrac{3}{2}(|z_1|^2+|z_2|^2)]\ . \tag{8.5c}$$

Amplitude equations of this form are familiar in Bénard convection[19–22] where n arises from vertical asymmetries such as thermal variations of fluid properties, distributed heat sources, or thermal modulation of the layer. Here n measures the degree of solute rejection. If our coordinates are chosen so that z_1 is real while z_2 and z_3 are conjugates, we find here, as in those convection problems, that there is subcritical bifurcation to hexagonal solutions which satisfy

$$z_1=\tfrac{3}{8}n\pm\left[\tfrac{9}{64}n^2+\frac{s}{2}\right]^{1/2},\quad s=\pm1\ , \tag{8.6}$$

$$|z_1|=|z_2|=|z_3|\ . \tag{8.7}$$

There is also supercritical bifurcation to rolls,

$$|z_i|^2=2,\quad |z_{j\neq i}|^2=0,\quad s=1\ . \tag{8.8}$$

Again, $s=+1$ (or -1) determines whether the solutions exist in the supercritical (or subcritical) range. The bifurcating sheet of hexagons is initially unstable but stabilizes at the limit point when $\mu=\mu_{-1}$ as shown in Fig. 8. The upper sheet remains stable until it loses stability at some $\mu_2>\mu_c$. Both bifurcating sheets of two-dimensional rolls are also initially unstable but stabilizes at some $\mu_1<\mu_2$ and remain stable as μ increases further. If conditions are near absolute stability and k is sufficiently near 1, then there exist stable, hexagonal interfaces when $\mu>\mu_c$. When $n>0$ (i.e.. $k>1$) z_1 is positive on the stable portion of the branch representing hexagonal solutions. In this case, the hexagons bulge outward into the melt. If, on the other hand, $n<0$ ($k<1$) then z_1 is negative and the stable hexagons are concave in the center. By calculating the solute distribution on the interface using (5.14), we find that solute concentrations are always maximum in the center of each hexagon. Therefore, these solutions represent hexagonal nodes[18] bulging into the melt when $k>1$ and dipping into the solid when $k<1$ but always with solute concentrations highest in the center of each hexagonal node. Finally, we note that the range of stable hexagons increases as n increases and the stabilization of the two-dimensional cellular solutions is postponed. As k varies from $k=1$, the transition at bifurcation is dominated by the appearance of hexagonal nodes.

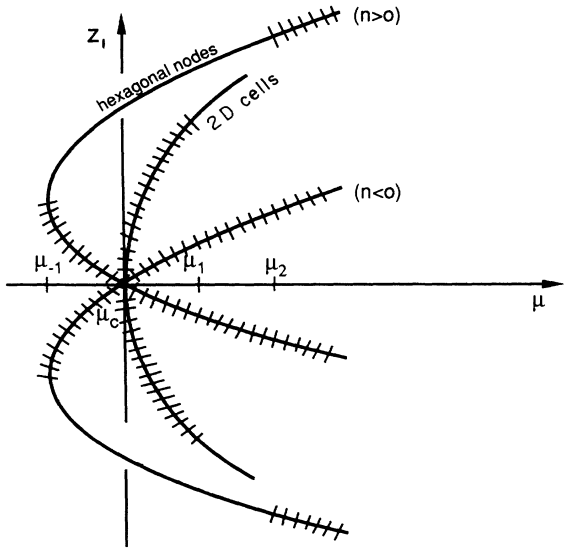

FIG. 8. Bifurcation diagram for the amplitude Eqs. (8.5). If $n>0$ (and $k>1$), the bifurcating hexagonal solutions bulge into the melt, and if $n<0$ ($k<1$), they dip into the solid. Hatched regions represent unstable solutions.

IX. CONCLUSION

A linear stability analysis on the planar growth of a directionally solidified binary alloy reveals[6] a short wavelength cutoff produced by surface tension; short wave disturbances are stable for all pulling velocities. As surface tension increases, longer waves are stabilized until a critical value is reached where the system is absolutely stable. We have shown that just below the limit of absolute stability, not only does the critical disturbance have a small wave number but so does every linearly unstable disturbance. As a result, our derivation of a long-wave evolution equation does not require pulling velocities to be near the critical value, and in this sense, the nonlinear evolution equation is strongly nonlinear. This property produces two interesting features. First, there is the appearance in the evolution equation of both quadratic terms, arising from solute rejection, and cubic terms due to the nonlinear effects of surface tension. Secondly, this equation has second-order time derivatives and time derivatives appearing in the nonlinear terms.

In Secs. VI–VIII, we studied features of the initial transition from planar to cellular states. We found from the evolution equation that two-dimensional supercritical stable cells are predicted. However, further analysis shows that these two-dimensional cells are unstable to three-dimensional instabilities. When the segregation coefficient k is near unity, these instabilities have hexagonal symmetries. When $k>1$, we find subcritical bifurcation to three-dimensional solutions with convex interfaces that correspond to hexagonal nodes. When $k<1$, we find subcritical bifurcation to three-dimensional solutions with concave interfaces that also correspond to hexagonal nodes. If k is near unity, this bifurcation has a limit point and a region of stable hexagonal solutions is found.

The onset of time dependence in directional solidification can arise through the development of sidebranching cells. There has also been experimental evidence[23] that other interesting time-dependent behavior may appear near absolute stability; cellular growth rates have been observed which are modulated in time. We would hope that the evolution equation, which is valid away from critical pulling rates, and has time derivatives that enter in a complicated way, might reveal a transition to these time-dependent states. This will be the object of future work.

Parameter regimes that allow a long-wave theory are especially attractive because the effects of additional physics are easily included. For example, the present theory may be modified to include the effects of attachment kinetics, anisotropy, and solutal convection, all of which may have an important role in the nonlinear development of cells near the limit of absolute stability. Latent heat, which may produce a considerable effect for large pulling velocities, can also be included using a long-wave approach.[2]

ACKNOWLEDGMENTS

This work was supported through a grant from the National Aeronautics and Space Administration Program on Microgravity Science and Applications.

[1]G. I. Sivashinsky, Physica **8D**, 243 (1983).
[2]A. Novick-Cohen and G. I. Sivashinsky, Physica **12D**, 253 (1984).
[3]G. W. Young and S. H. Davis, Phys. Rev. B **34**, 3388 (1986).
[4]G. W. Young, S. H. Davis, and K. Brattkus, J. Cryst. Growth **83**, 560 (1986).
[5]A. Novick-Cohen, Physica **26D**, 403 (1987).
[6]W. W. Mullins and R. F. Sekerka, J. Appl. Phys. **35**, 444 (1964).
[7]A. Novick-Cohen (unpublished).
[8]D. J. Wollkind and L. A. Segel, Philos. Trans. R. Soc. London, Ser. A **268**, 351 (1970).
[9]J. M. Hyman, A. Novick-Cohen, and P. Rosenau, Phys. Rev. B **37**, 7603 (1988).
[10]D. A. Kurtze, Phys. Rev. B **37**, 379 (1988).
[11]J. S. Langer, Rev. Mod. Phys. **52**, 1 (1980).
[12]D. J. Wollkind, R. Sriranganathan, and D. B. Oulton, Physica **12D**, 215 (1984).
[13]J. T. Stuart, J. Fluid Mech. **9**, 353 (1960).
[14]A. C. Newell and J. A. Whitehead, J. Fluid Mech. **38**, 279 (1969).
[15]L. A. Segel, J. Fluid Mech. **38**, 203 (1969).
[16]L. H. Ungar and R. A. Brown, Phys. Rev. B **29**, 1367 (1984).
[17]G. B. McFadden and S. R. Coriell, Physica **12D**, 253 (1984).
[18]G. B. McFadden, S. R. Coriell, and R. F. Boisvert, J. Cryst. Growth **84**, 371 (1987).
[19]L. A. Segel, J. Fluid Mech. **21**, 359 (1965).
[20]F. H. Busse, J. Fluid Mech. **30**, 625 (1967).
[21]R. Krishnamurti, J. Fluid Mech. **33**, 457 (1968).
[22]M. N. Roppo, S. H. Davis, and S. Rosenblat, Phys. Fluids **27**, 796 (1984).
[23]W. J. Boettinger, D. Shechtman, R. J. Schaefer, and F. S. Biancaniello, Met. Trans. **15A**, 55 (1984).